13B.2 COMPARISON OF SELECTED IN-SITU AND REMOTE SENSING TECHNOLOGIES FOR ATMOSPHERIC HUMIDITY MEASUREMENT

Petteri Survo*[1], Thierry Leblanc[2], Rigel Kivi[3], Hannu Jauhiainen[1], Raisa Lehtinen[1,]
[1]Vaisala Oyj, Helsinki, Finland, [2] California Institute of Technology, Jet Propulsion Laboratory, Wrightwood, California, [3]Finnish Meteorological Institute, Arctic Research, Sodankylä, Finland

1. INTRODUCTION

Present-time operational radiosondes are able to produce atmospheric humidity observations with high resolution and precision, but remote sensing technologies have also shown good progress in producing more detailed humidity profiles with reasonably small uncertainties. In addition, several remote sensing methods can provide accurate integrated precipitable water (IPW) column data for meteorological purposes. As the accuracy of both numerical weather prediction models and global climate models is largely dependent on the quality of the available water vapor pressure data, Joo (2013), Singh (2014), GCOS-112 (2007), it was seen relevant to comparatively evaluate the performance of the latest in-situ and remote sensing technologies.

In this study, the humidity measurements of Vaisala Radiosondes RS92 and RS41 are compared against water vapor pressure profiles measured with a high-capability water vapor Raman LIDAR, situated at Jet Propulsion Laboratory Table Mountain Facility in California, USA. Another performance analysis was made by comparing the IPW values calculated from the radiosonde relative humidity measurements to simultaneous IPW measurements of microwave radiometers and GPS receivers at the same site. Comparative soundings were also conducted at the Arctic Research Center of Finnish Meteorological Institute in Sodankylä, Finland. In these soundings, a Cryogenic Frostpoint Hygrometer (CFH) was applied as an in-situ reference instrument.

2. DIFFERENCES IN VAISALA RADIO-SONDE RS92 AND RS41 HUMIDITY MEASUREMENT TECHNOLOGIES

Vaisala Radiosondes RS92 and RS41 participated in both Table Mountain and Sodankylä intercomparison campaigns. Thus, even though the focus of this study is in comparing the performance of a diverse set of instruments for atmospheric humidity measurement, it also gives valuable information of how the humidity measurement of RS92 and RS41 differs at the climate conditions of the chosen test sites.

The differences in Vaisala Radiosonde RS92 and RS41 pressure, temperature, and humidity measurements have been studied in sounding campaigns arranged at various climate conditions, see Edwards (2014), Vaisala (2014, 2013). In general, the observed mutual mean deviations have been moderate, while there is a positive development found in the consistency of the measurements. In the case of RS41 humidity measurement, the improved precision is mainly a result of two factors: 1) The new sensor chip design with an integrated temperature sensor reduces uncertainties due to varying solar and IR radiation conditions. 2) The RS41 in-built sensor checks are highly independent of external factors, such as the ambient conditions or the operator's procedures during the ground preparations. The key differences of the two radiosonde models are summarized in Table 1.

Radiosonde	RS41-SG	RS92-SGP
Sensor type	Thin-film capacitor, integrated T sensor and heating functionality	Thin-film capacitor, heated twin sensor
Combined uncertainty in sounding (k=2)	4 %RH	5 %RH
Response time (63.2 %, 6 m/s flow, 1000 hPa)	< 0.3 s, +20 ºC < 10 s, -40 ºC	< 0.5 s, +20 ºC < 20 s, -40 ºC
Ground check	Corrected with RS41 in-built Physical Zero Humidity Check in ambient air	Corrected against 0%RH humidity generated by desiccants

Table 1. The key differences of RS41 and RS92 humidity measurements.

* *Corresponding author address : Petteri Survo, Vaisala Oyj,* P.O. Box 26, FI-00421 Helsinki, Finland, *e-mail: petteri.survo@vaisala.com

In the sounding campaigns discussed in this paper, the Vaisala radiosonde results were calculated using DigiCORA® sounding system MW31 software version 3.66 for RS92 and DigiCORA® sounding system MW41 software version 2.1 for RS41.

3. TABLE MOUNTAIN INTERCOMPARISON CAMPAIGN

NASA Jet Propulsion Laboratory (JPL) Table Mountain Facility is located near Wrightwood, CA, in the Angeles National Forest at the elevation of 2285 meters. Three remote sensing instruments of the facility were involved in the inter-comparison: A high-capability water vapor Raman LIDAR, profiling humidity up to 20 km, and a GPS receiver system and a microwave radiometer instrument measuring integrated precipitable water (IPW) columns. During the campaign period, 2014-05-29 - 2014-10-30, a total of 19 dual soundings were conducted using Vaisala Radiosondes RS92 and RS41. At the time of measurements, the weather conditions were typically dry and the sky conditions clear.

Figure 1. NASA Jet Propulsion Laboratory Table Mountain Facility.

3.1 *Ground-based Instruments Involved*

The ground-based instruments applied in the study are presented here in brief. More elaborate instrument descriptions can be found in the reports by Leblanc (2011, 2012).

The Raman LIDAR

The high-capability Raman LIDAR of the Jet Propulsion Laboratory (JPL) was taken into use in 2005. Since then, constant instrument development has been done, resulting in the implementation of some significant upgrades, see Leblanc (2012). At present, the LIDAR comprises a Nd:YAG laser with a high-pulse energy of 650 mJ at 355 nm, a large telescope 0.91 m in diameter, and 4 small telescopes. The operating principle of the water vapor Raman LIDAR is to transmit laser pulses to the atmosphere and to collect back-scattered signals at wavelengths that are Raman-shifted by nitrogen (387 nm) and water vapor (407 nm). The ratio of the corrected signals is proportional to the water vapor mixing ratio in the atmosphere. A profile is produced by sampling signals in time, and the achieved vertical resolution ranges from 150 to 900 m depending on the altitude and the applied channel, and extends over 1 km at altitudes above 12 km. Due to the measurement principle, Raman LIDAR is operated at night-time and preferably in clear sky conditions. In the campaign, the LIDAR profiles were calibrated using the RS92 Miloshevich-corrected data typically between 3 km and 6 km, see Miloshevich (2004, 2009). The JPL Table Mountain LIDAR has a demonstrated capability to measure water vapor profiles from ~1 km above the ground to the lower stratosphere with a precision of 10% or better near 13 km and below, and an estimated accuracy of 5 %, as discussed by Leblanc (2012).

GPS-based IPW

The GPS IPW instrument at the Table Mountain facility is operated by NOAA Forecast Systems Laboratory. The measurement of the integrated precipitable water (IPW) column with the GPS receivers is based on observing the time delay, i.e., a phase shift, that the atmospheric water vapor generates to the GPS satellite radio signal. The instrument outputs IPW results at a 30 minutes' time resolution in a continuous operational mode and has an estimated measurement uncertainty of 1.5 mm + 1 % in column water.

Micro Wave Radiometer

At the Table Mountain site, the Micro Wave Radiometer (MWR) instrument is ran by Naval Research Laboratory. Microwave radiometers determine the IPW column height by measuring the emissions from the water molecule's rotational transitions at a 22 GHz range. This instrument also operates on continuous basis with a time resolution of 30 - 35 minutes. The estimated uncertainty of the MWR instrument is 3% in column water.

3.2 *Results*

Humidity Profiles

The humidity measurements of Vaisala radiosondes are modeled and calibrated using relative humidity (RH) as the primary measurand. In this study, the RH results were converted to water vapor volume mixing ratio (WV VMR) using Wexler's saturated water vapor pressure formulations updated by Hardy (1998). Respectively, as needed, the WV VMR results of the LIDAR were converted to relative humidity using RS92 temperature observations and Hyland and Wexler (1983) formulas. Deviations between the two saturated water vapor pressure formulas are less than 1% over the temperature range of interest, and, thus, considered not to have a significant impact on the interpretation of the results.

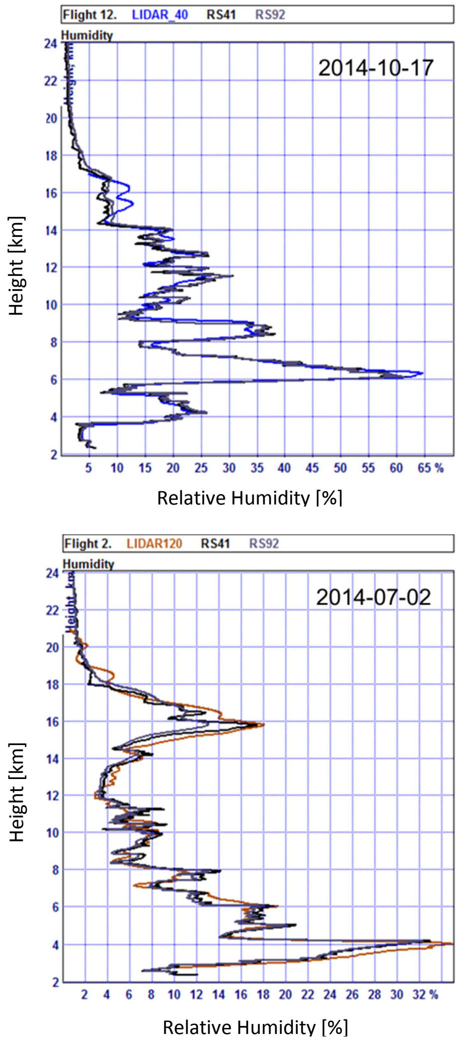

Figure 2. Examples of relative humidity profiles measured with Vaisala Radiosondes RS41 (black), RS92 (gray) and the JPL Raman LIDAR - The LIDAR signals averaged for 40 min. (blue, top) and for 120 min. (brown, bottom).

To present LIDAR humidity profiles, two averaging times of the signals were applied. The 40-minute averaging time corresponds roughly to the time period of a balloon's ascend to 10 km, and the 120-minute averaging time matches a typical duration of a complete sounding. A longer averaging time suppresses measurement noise, and thus extends the detecting range to higher elevations.

Figure 2 illustrates relative humidity profiles from the Table Mountain campaign, the three instruments typically demonstrating very good agreement.

The statistical summary of all 17 simultaneous relative humidity profiles calculated with the RSKOMP sounding analysis software is presented in Figure 3. Here the profiles of each sounding were first manually synchronized in an altitude scale, and a 0.5-km vertical resolution was applied in the analysis.

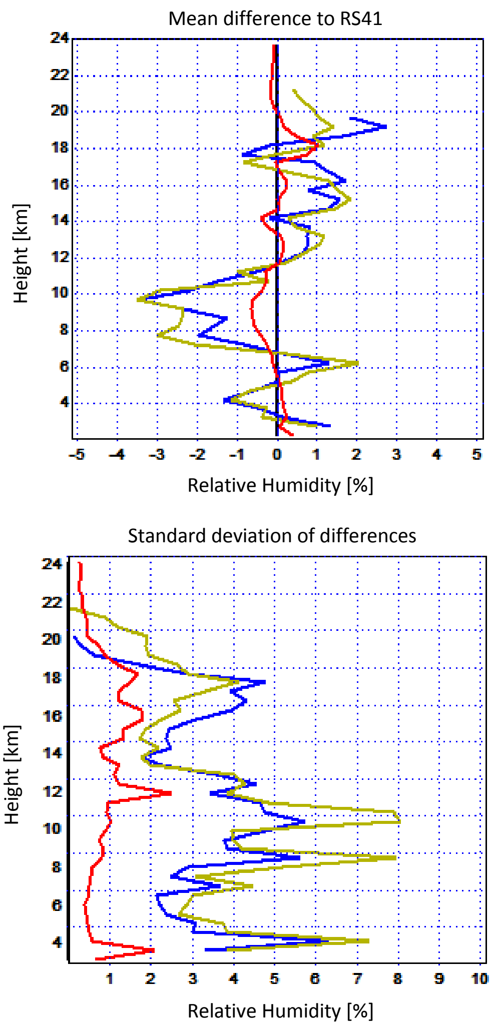

Figure 3. Statistical summary of relative humidity results: Mean differences to radiosonde RS41 (top) and standard deviations of differences (bottom) - RS92 (red), LIDAR averaged for 40 min. (blue) and 120 min. (olive).

The analysis shows that the two radiosonde measurements agree within 1 % RH over the whole altitude range, and standard deviations of differences typically stay under 2 % RH. As the

LIDAR results are compared to the RS41 measurement, the agreement is typically better than 2 % RH, while some larger deviations are observed at the altitude range of 8-10 km. As a rule, the standard deviations range from 2 to 6 % RH for the 40-minute averaged signal. Apparently the temporal mismatch of the 120-minute averaged LIDAR signal and the sounding measurements leads to an increase of incidental deviations between the two instruments, even on average the results agree quite as well as those of the shorter signal averaging.

An example of the humidity profiles expressed in the volumetric water vapor mixing ratio is shown in Figure 4. This also demonstrates the fine resolution and accordance of the instruments.

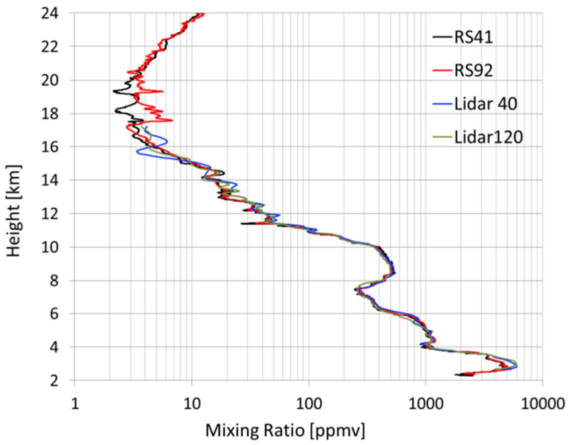

Figure 4. Sounding #11 illustrating volumetric mixing ratio profiles from Table Mountain, date 2014-10-14.

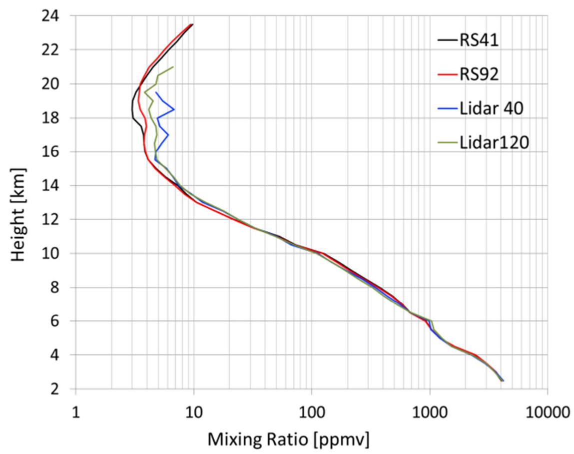

Figure 5. Mean profiles of 17 simultaneous humidity measurements expressed as volumetric mixing ratio.

Mean profiles in water vapor volume mixing ratio were calculated with the RSKOMP software using a 0.5-km vertical resolution, see Figure 5.

When comparing the mean profiles of the two radiosonde models, the differences are typically smaller than 5 % of the mixing ratio below 17 km and less than 20 % above 17 km. Relative to RS41, the humidity profiles of RS92 tend to dry slightly more slowly from more humid conditions of the tropopause to the stratospheric low-humidity levels, and this is seen in the mean profile differences at the altitude range of 17 – 20 km.

In the volumetric mixing ratio analysis, the LIDAR measurements averaged for 40 minutes typically agree with RS41 within 10 % up to 14 km, and within 20 % up to 16 km. There are larger deviations observed in the vicinity of the tropopause region, 16 - 20 km in altitude, which is, at least partly, due to the increased uncertainties in detecting profile shapes in these challenging conditions – cold temperature leads to larger time lag corrections for the radiosondes and the vertical resolution of the LIDAR results extends already to 3.6 km. The LIDAR measurements averaged for 120 minutes show a bit larger deviations at troposphere region, but agree better with the radiosondes above 16 km, as can be expected.

Integrated Precipitable Water Columns

Generally speaking, the IPW column value is dominated by the moisture content of the lower troposphere, which is evident based on the mixing ratio profiles of Figures 4 and 5. In case of radiosonde measurements, the integrated precipitable water (IPW) column heights were derived from the relative humidity and temperature profiles using the saturated water vapor pressure formula of Hardy (1998) and the general expression for the water vapor density. GPS and MWR instruments output IPW values about every 30 minutes at their own pace, and that is why the results had to be synchronized with the soundings. This was done by fitting two IPW estimators, one at the launch time and another at launch time + 30 minutes, to the time series of IPW data, and using the average of the estimator values. With the average ascend rate in the soundings, 3.9 m/s, the 30 minutes' sampling period corresponds to a 7.0-km rise in altitude. This coincides with the most humid layer of the lower troposphere, and, thus, the procedure should enable a valid IPW column comparison of the different measurement technologies.

For the comparative analysis of IPW results, a total of 18 measurements were available by the GPS instrument and 16 measurements by the

MWR, presented in Figure 6. As a general observation of the results, it can be noted that the climate conditions at Table Mountain site are relatively dry. The average column height was just 6.0 mm, as it can be over ten-fold in the tropics. In the graphical analysis of Figure 6, the GPS measurement was used as a reference (x-axis). The IPW columns calculated from the two radiosonde measurements show almost one-to-one correlation with the GPS columns, RS41 demonstrating a slightly better agreement. There is a single outlier in the results of microwave radiometer measurements and omitting that from the analysis would have resulted in an equally good correlation.

Standard deviations of each IPW measurement occasions average out 0.46 mm in column water, which also indicates a distinct accordance between the four instruments.

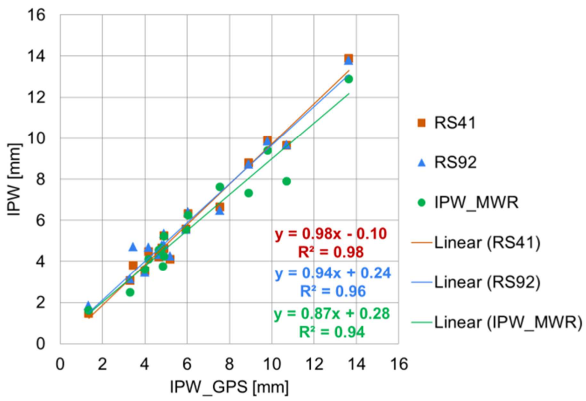

Figure 6. Integrated Precipitable Water column results derived from the sounding profiles of RS41 and RS92, and the results of MWR compared with the results of the GPS instrument. Equations of linear fit and coefficients of determination are indicated by the color of data series.

4. SODANKYLÄ INTERCOMPARISON CAMPAIGN

The Arctic Research Center of Finnish Meteorological Institute in Sodankylä is situated in northern Finland, about 100 km north from the polar circle. During the campaign period, 2014-02-07 - 2014-11-19, a total of 6 soundings were launched where operational radiosondes RS92 and RS41 were compared against a reference grade Cryogenic Frostpoint Hygrometer (CFH) instrument. To ascertain the reliability of the results, the CFH instrument is preferably operated avoiding wet cloud conditions. Therefore, during the time of the measurements the conditions were typically dry, though high clouds were present in some of the soundings.

Figure 7. A launch of a sounding at the Arctic Research Center of Finnish Meteorological Institute in Sodankylä. CFH and ozone instruments are located in the middle of the rig, radiosondes at both ends of the rig.

4.1 *Cryogenic Frostpoint Hygrometer*

CFH is a well-established and commonly accepted reference instrument for atmospheric humidity measurements. It is a chilled mirror hygrometer, that is, in operation it optically detects the amount of frost on its temperature-controlled mirror surface, and when the frost layer is stable, the mirror temperature directly indicates the prevailing frostpoint temperature of the sampled gas. The uncertainty of the instrument is estimated to be 0.5 °C in frostpoint temperature, and it is one of the few instruments capable of measuring the low-water vapor levels in the mid-stratosphere, see Vömel (2007).

4.2 *Results*

In the analysis of the radiosonde humidity results, the unit conversion routines were applied as presented in Chapter 3.2. For the conversion of CFH frostpoint readings to relative humidity and volumetric mixing ratio, radiosonde RS41 temperature and pressure results were used when applying the saturated water vapor pressure formulas of Hardy (1998) and the general RH and WV VMR equations.

Figures 8 and 9 present illustrative relative humidity profiles measured over the course of the Sodankylä campaign. In the two soundings, the good accordance of the instruments is clearly visible. Furthermore, an interesting observation can be made when studying the summer and winter-time mid-stratospheric humidity results. In the summer-time profile, presented in Figure 8, the temperature at 25 km height is about -46 °C and, according to CFH, the relative humidity is about 0.1 %. Obviously the operational radiosondes also demonstrate good performance, showing readings well under 1 % RH, even if the relative deviation to CFH is significant. In the winter-time graph shown in Figure 9, the stratosphere temperature around 25 km is as low as -85 °C, and even though there is no notable change in the absolute humidity level (about 5 ppmv), the relative humidity by CFH is at level of 18 %. A noteworthy fact is that this substantial increase in RH is also observed by radiosonde RS41 and the results agree well with the CFH instrument.

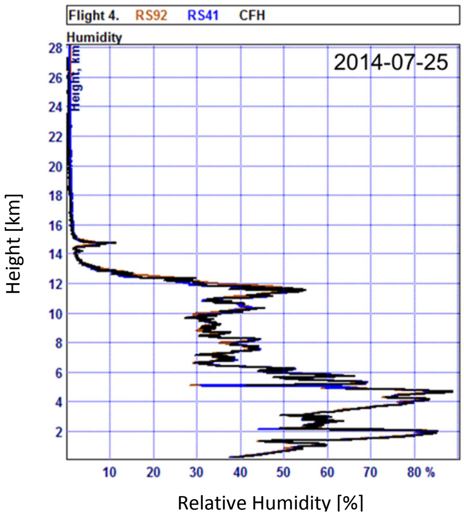

Figure 8. A relative humidity profile from Sodankylä measured with Vaisala Radiosondes RS41 (blue), RS92 (brown) and CFH (black) in the summer time.

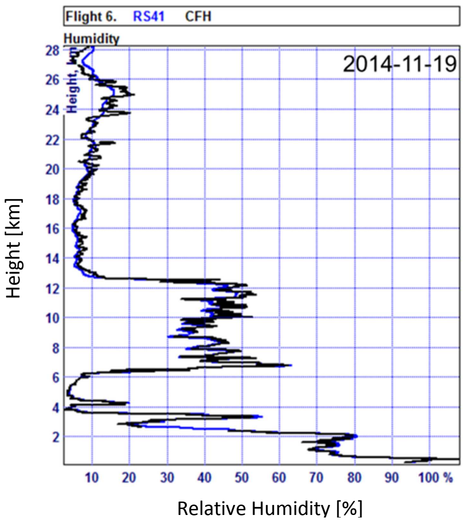

Figure 9. A winter-time relative humidity profile from Sodankylä measured with Vaisala Radiosonde RS41 (blue) and CFH (black).

A statistical summary of the relative humidity profiles measured in Sodankylä is presented in figure 10. A vertical resolution of 0.5 km was applied in the analysis conducted with the RSKOMP software.

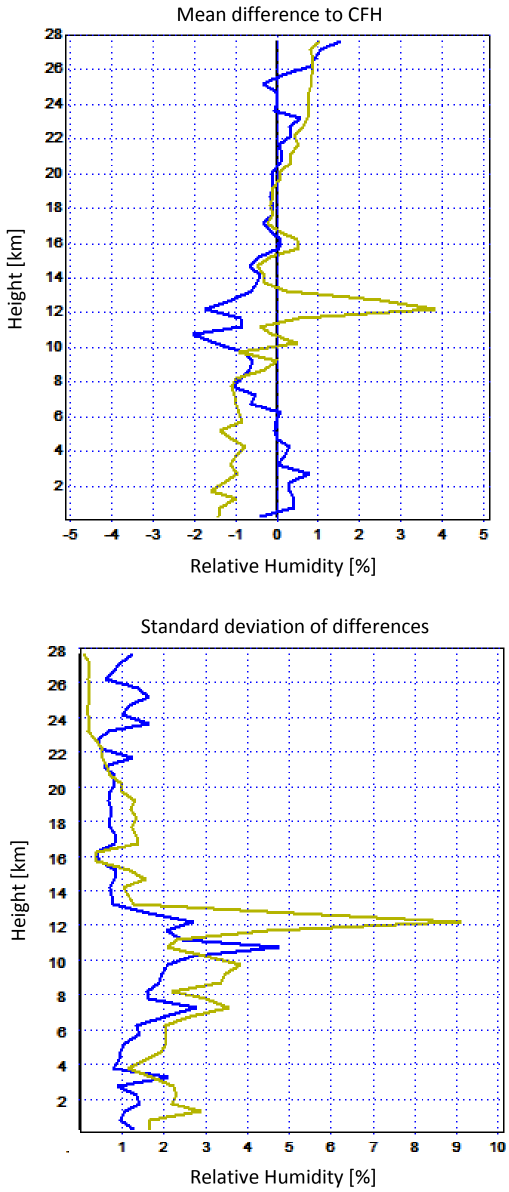

Figure 10. Statistical summary of relative humidity results: Mean differences to CFH (top) and standard deviations of differences (bottom) - RS92 (olive), RS41 (blue).

According to the analysis, the mean differences between the CFH and RS41 results are typically less than 1 % in RH, and larger deviations are observed mainly at the dynamic measurement conditions in the vicinity of the tropopause. The results of RS92 are typically 1 % RH lower than those of CFH at the lower and mid-troposphere altitudes. However, at the tropopause, around 12 km in altitude, RS92 shows more moist readings. This moderate positive deviation seems to be related to the slower drying of RS92 readings to the low stratospheric levels after the humid tropopause phase.

For RS41, the standard deviations of RH differences to CFH increase gradually along with the altitude, from 1 % RH close to the ground to a peak of over 4 % RH close to the tropopause, and then settle to a level of around 1 % in the stratosphere. The shape of the variation graph of RS92 resembles the RS41's graph with the exception that the amount of variation is typically 1 % RH higher in the troposphere and the peak at the tropopause is more pronounced.

Figure 11 presents an example of water vapor profile expressed in volumetric mixing ratio. The graphs show that in the troposphere, all the instruments measure with a good agreement, but above 12 km, the operational radiosondes show significantly higher mixing rate values, even though in relative humidity the deviations are less than 1 % RH.

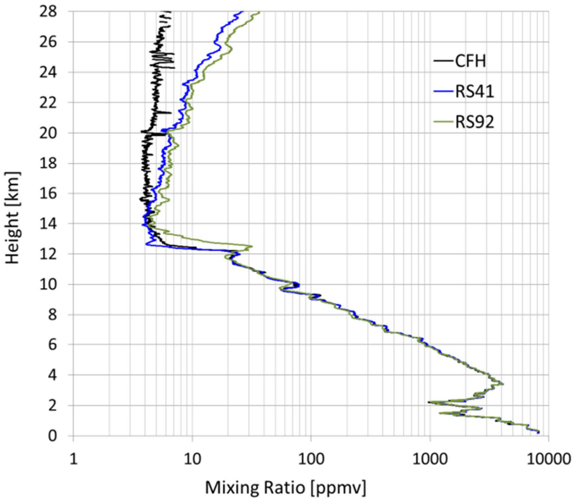

Figure 11. Sounding #5 illustrating volumetric mixing ratio profiles from Sodankylä, date 2014-10-03.

Mean profiles in WV VMR were calculated with the RSKOMP software using a 0.5-km vertical resolution, as shown in Figure 12.

The mean profile of RS41 agrees within 2 % in WV VMR up to 12 km and within 10 % up to 15 km, when compared with the CFH profile. And when comparing RS92 to CFH, the mean deviations are typically in the range of 1 - 4 % in mixing ratio up to 11 km. Hence, both operational radiosondes demonstrated very good performance in these high-latitude climate conditions. However, the WV VMR results of the stratosphere part of the profile indicate that of the instruments participating the comparison, only CFH was capable of measuring the stratospheric very-low humidity levels with firm consistency, even though the operational radiosondes performed well at relative humidity scale.

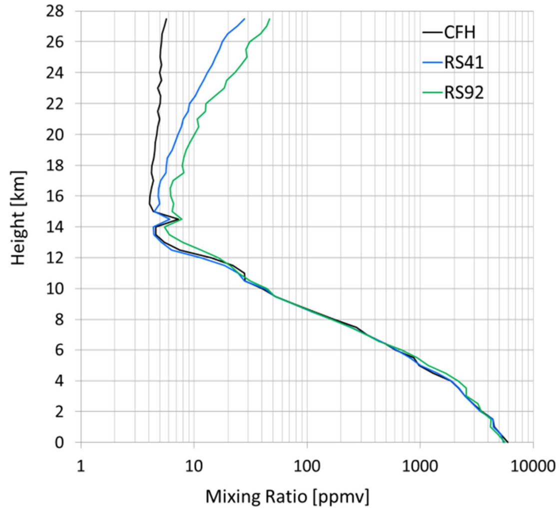

Figure 12. Mean profiles of simultaneous humidity measurements expressed in volumetric mixing ratio. Sample size is 6 for CFH and RS41, 5 for RS92.

5. SUMMARY

The intercomparison campaigns of atmospheric in-situ and remote sensing water vapor instruments were arranged at the NASA Jet Propulsion Laboratory Table Mountain Facility in California and at the Arctic Research Center of Finnish Meteorological Institute in Sodankylä, northern Finland. The campaign sites represented two different climate conditions, though the typical humidity profiles were relatively dry in both locations.

When comparing the water vapor volumetric mixing ratio mean profile of the LIDAR measurements averaged for 40 minutes with the mean profile of Vaisala Radiosonde RS41, the agreement was typically within 10 % up to the altitude of 14 km. From 14 km up to 20.5 km, the mixing ratio results were at a range of 3 - 8 ppmv, and the deviations between the instruments ranged from 0.5 to 1.5 ppm, as the 120-minute averaging was used for the LIDAR.

In the comparison of integrated precipitable water column measurements, the ground-based observations of the GPS IPW and the microwave radiometer instrument, as well as the radiosonde derived water columns of RS92 and RS41, typically all agreed within 1 mm.

The in-situ instrument comparison of CFH and Vaisala Radiosonde RS41 resulted in mean humidity differences that were typically smaller than 1 % RH. A winter-time arctic profile revealed the capability of RS41 to measure risen relative humidity levels at the extremely cold stratosphere. The mean volumetric mixing ratio profiles of the two instruments agreed within 2 % in VMR up to 12 km and within 10 % up to 15 km. In measuring the extremely low absolute humidity levels of the stratosphere, CFH demonstrated the highest performance.

In the dual soundings conducted during the Table Mountain campaign, the mean differences between the Vaisala Radiosondes RS92 and RS41 were smaller than 1 % RH. Respectively, in the Sodankylä campaign, the deviations were typically within 2 % RH, RS92 showing slightly lower values in the troposphere, and higher values while measuring the fast drying humidity profiles at the tropopause.

ACKNOWLEDGMENTS

We thank Seth Gutman and Kirk Holub from NOAA Forecast Systems Laboratory for providing GPS-based IPW data, and Gerald Nedoluha from Naval Research Laboratory for providing Microwave radiometer data for the study.

6. REFERENCES

CGOS-112 (WMO/TD No. 1378), April 2007: GCOS Reference Upper-Air Network (GRUAN), Justification, requirements, siting and instrumentation options

Hardy, B., 1998, ITS-90 Formulations for Vapor Pressure, Frostpoint Temperature, Dewpoint Temperature, and Enhancement Factors in the Range –100 to +100 °C, The Proceedings of the Third International Symposium on Humidity & Moisture, London, England

Joo, S., J. Eyre, R. Marriott, 2013: The Impact of MetOp and Other Satellite Data within the Met Office Global NWP System Using an Adjoint-Based Sensitivity Method. Mon. Wea. Rev., 141, 3331–3342.

Leblanc, T., T. D. Walsh, I. S. McDermid, G. C. Toon, J.-F. Blavier, B. Haines, W. G. Read, B. Herman, E. Fetzer, S. Sander, T. Pongetti, D. N. Whiteman, T. G. McGee, L. Twigg, G. Sumnicht, D. Venable, M. Calhoun, A. Dirisu, D. Hurst, A. Jordan, E. Hall, L. Miloshevich, H. V¨omel, C. Straub, N. Kampfer, G. E. Nedoluha, R. M. Gomez, K. Holub, S. Gutman, J. Braun, T. Vanhove, G. Stiller, A. Hauchecorne, 2011, Measurements of Humidity in the Atmosphere and Validation Experiments (MOHAVE)-2009: overview of campaign operations and results Atmospheric Measurement Techniques, 4, 2579–2605

Leblanc, T., I. S. McDermid, and T. D. Walsh, 2012, Ground-based water vapor raman lidar measurements up to the upper troposphere and lower stratosphere for long-term monitoring, Atmospheric Measurement Techniques, 5, 17–36

Miloshevich, L. M., Paukkunen, A., V¨omel, H., and Oltmans, S. J., 2004: Development and Validation of a Time-Lag Correction for Vaisala Radiosonde Humidity Measurements, J. Atmos. Ocean.Technol., 21, 1305–1327.

Miloshevich, L. M., V¨omel, H., Whiteman, D. N., and Leblanc, T., 2009: Accuracy assessment and correction of Vaisala RS92 radiosonde water vapor measurements, J. Geophys. Res., 114, D11305, doi:10. 1029/2008JD011565.

Singh, R., S.P. Ojha, C. M. Kishtawal, P. K. Pal, 2014: Impact of various observing systems on weather analysis and forecast over the Indian region, Journal of Geophysical Research: Atmospheres, Vol. 119, Issue 17, 10,232–10,246

Edwards, D., G. Anderson, T. Oakley, P. Gault, 2014: UK MET Office Intercomparison of Vaisala RS92 and RS41 Radiosondes

Vaisala, 2014: Vaisala RS41 Trial in the Czech Republic, Vaisala News 192/2014, pages 14 – 17

Vaisala, 2013, Comparison of Vaisala Radiosondes RS41 and RS92, White Paper

Vömel, H., 2007, D. E. David, K. Smith, Accuracy of tropospheric and stratospheric water vapor measurements by the cryogenic frost point hygrometer: Instrumental details and observations, J. Geophys. Res.,112, D08305, doi:10.1029/2006JD007224